14

Analysis of the suitability of a scintillation detector LSO for clinical dosimetry

© S.A. Yagnyukov,[1] J.S. Lebedeva,[1] D.M. Blitman,[2] O.V. Yurasova[2]

[1] Pavlov First St. Petersburg State Medical University,
197022 St. Petersburg, Russia
[2] Federal State Research and Development Institute of
Rare Metal Industry („Giredmet") JSC,
111524 Moscow, Russia
e-mail: seomcka.seom@yandex.ru

Received October 25, 2025
Revised December 17, 2025
Accepted January 10, 2026

The possibility of using scintillation detectors based on LSO crystals (Lu_2SiO_5:Ce) for the tasks of clinical dosimetry in radiotherapy. A computer simulation of the process of photon generation and registration in a scintillation detector in the Geant4 program has been performed, and optimal crystal parameters (length 10−15 mm for photon energy 1.25−7.5 MeV) have been determined. An experimental test of the prototype detector in a water phantom at the Varian Unique accelerator revealed its advantages (spatial resolution comparable to that of the Sun Nuclear EDGE semiconductor detector) and disadvantages (sensitivity to illumination, nonlinear dependence on radiation power). The results confirm the possibility of using scintillators in dosimetry, however, existing detectors have an advantage due to the smaller thickness of the detector and, consequently, less influence on the uniformity of the radiation flux.

Keywords: clinical dosimetry, scintillator, computer simulation, experimental verification.

DOI: 10.61011/TP.2026.04.63278.296-25

Introduction

Modern radiotherapy is one of the key methods of curing oncological diseases, since it provides local impact of ionising radiation (IR) on tumor tissues with minimum damage to healthy structures. But efficiency and safety of radiotherapy directly depend on accuracy of dosimetry, i.e. measurement and control of distribution of an absorbed dose in biological tissues. Traditionally, ionization chambers and semiconductor detectors are applied in clinical practice, but these technologies have some limitations that include insufficient spatial resolution, a dependence on the temperature and complexity of operation.

Scintillation detectors designed to convert IR into optic radiation have a high potential for improving dosimetry systems. Their advantages include high sensitivity, miniaturizability and no need for external power supply for operation of a scintillator. They can be applied when submillimeter accuracy of measurements is required, where the ionization chambers (which are a standard of the modern dosimetry) can not provide required accuracy of measurements due to limitations to volume reduction. A coupling of the scintillator and a photodiode potentially can generate a current that is in 5−10 times higher with the similar volumes, making it possible to reduce a crystal size without deteriorating a signal-to-noise ratio and to improve accuracy of dosimetry.

Despite successful use of LSO crystals (Lu_2SiO_5:Ce) in positron-emission tomography (PET), their use in clinical dosimetry is understudied. In particular, there are no data about optimal geometry of the crystal for various energies of therapeutic beams, influence of design specific features of the detector (for example, a length of an optical fiber) on measurement accuracy and comparative efficiency of the scintillation detectors in relation to traditional systems under conditions of a water phantom.

The present study is aimed at estimating suitability of the LSO-based scintillation detectors for clinical dosimetry via complex simulation and experimental verification. The aim was achieved by solving the following problems:

1) analysis of the characteristics of the LSO scintillator for verifying creatability of the detector based thereon;

2) computer simulation in Geant4 for determining:

- a dependence of light output on the crystal length at energies 500 keV−7.5 MeV;
- light losses in a PMMA optical fiber (polymethyl methacrylate) of a different thickness;

3) experimental verification of a detector prototype:

- measurement of linearity of a response, noise characteristics and afterglow;
- comparison with the semiconductor detector Sun Nuclear EDGE and the ionization chamber SNC125 in the water phantom.

A scientific novelty of the study consists of the first systematic analysis of application of the LSO scintillator for dosimetry of the therapeutic beams, designing a methodology of optimization of detector geometry based on simulation and of identifying key design limitations.

1. Review of references

Modern studies in the field of scintillation materials for medical dosimetry demonstrate a growing interest to cerium-doped scintillation crystals, in particular, Lu_2SiO_5:Ce, which is due to a unique combination of its physical and operating characteristics. Analysis of literature data makes it possible to distinguish key advantages of the selected scintillator as compared to the traditional ones such as NaI(Tl), BGO or CsI(Tl). A matter of principle is applied to: a high density of the material, a short radiation length and high light yield, which provide effective absorption of IR therapeutic doses within a compact crystal volume, which is crucial for miniaturizing medical-purpose detectors. LSO has the density of 7.4 g/cm^3, the radiation length of 1.14 cm and light yield of 30 photon/keV. Besides, it is not hygroscopic [1–5].

LSO has high radiation resistance: light yield is reduced by less than 10 % when the crystal receives the dose of 2000 Gy [6]. When using in monthly dosimetry in a Varian Unique accelerator, this dose will be obtained by the detector for 1.5−2 years of operation.

In combination with absence of hygroscopicity, temperature stability of LSO that demonstrates a deviation of light yield by no more than 1.5 % in a clinically significant range 285−300 K radically differentiates this material from common hygroscopic scintillators of the NaI(Tl) type, which require hermetic packaging [7]. The most important characteristic to be applied in real time is a short fluorescence lifetime: LSO — 40 ns, which by an order exceeds the similar parameter for CsI(Tl) — 1220 ns and makes it possible to minimize a signal overlapping effect when manipulating pulsed beams of modern medical accelerators. At the same time, energy resolution of LSO (662 keV) is 6.89 %, thereby meeting requirements of clinical dosimetry [8].

Special attention should be paid to successful introduction of LSO into commercial systems of medical visualization, such as PETCT scanners Philips Vereos, Siemens Biograph Vision and Biograph Vision Quadra, in which these crystals provide record-breaking spatial resolution, thereby confirming their technological maturity and reproducibility of the characteristics in serial production [9–14]. LSO is considered as promising options of miniature matrices with high resolution for PET-CT visualization of small animals [15–17]. This scintillator also demonstrates better efficiency as compared to other nonorganic modern scintillators when recording single gamma photons of 2.22 MeV [18].

However, analysis of the literature detects a considerable gap in studied exactly dedicated to dosimetric applications of LSO, since most studies are focused on visualization tasks, thereby making the present study especially relevant for filling in this niche and extending the fields of application of these materials.

Comparative analysis of the characteristics of various scintillators unambiguously indicates advantages of LSO in a set of parameters that are important for clinical dosimetry: the high density and an effective atomic number provide good efficiency of recording high-energy radiation, while temperature stability guarantees reproducibility of results in real clinical conditions.

Technological difficulties of growing large LSO single crystals and their relatively high cost as compared to the traditional materials are still factors that limit wide-scale implementation. But a progress in synthesis methods and cost-reduced production, which are observed in Russia in recent years, make it possible to predict expansion of application of these materials in the medical dosimetry.

The performed analysis of the literature confirms that LSO is a promising option for designing new-generation scintillation detectors of clinical dosimetry, which combines optima physical characteristics. Absence of systematic studies of its dosimetric capabilities under conditions of the water phantom makes the present study timely and practically significant for designing methods of precise radiotherapy.

2. Methods

2.1. Computer simulation in Geant4

The scintillation detector was simulated using the Geant4 software of the 11.1.3 version, which was chosen due to its capability of simulating nuclear interactions and optical processes, thereby making it possible to accurately describe the detector geometry, properties of its components and experimental conditions.

The geometrical model includes several basic components: air-filled volume of a calculation domain of the size $50 \times 10 \times 10$ mm, the LSO scintillator shaped as a rectangular parallelepiped with variation of length from 4 to 32 mm with a step of 1 mm at the constant cross-section 3×3 mm; the PMMA optical fiber of the 1 mm diameter and the 120 cm length with a refractive index of 1.49; as well as an idealized detector with a sensitive area 3×3 mm and 100 % efficiency. The system of coordinates was arranged so that the X axis corresponded to the beam direction and the longitudinal axis of the crystal, while an origin of coordinates was at a point, where the photon entered the crystal.

A radiation source was simulated as a photon ray with monochromatic lines at the energies 511 keV, 1.25, 3, 5 and 7.5 MeV, which was normally falling onto an end face of the crystal; in doing so, both axial as well as lateral detection was considered.

With each energy and crystal length, it included from 10 000 to 20 000 simulations. Data were analyzed by calculating efficiency of recording via finding a maximum of the dependence of light output on the crystal length.

2.2. Experimental verification

An experimental part of the study included complex verification of the designed scintillation detector in real

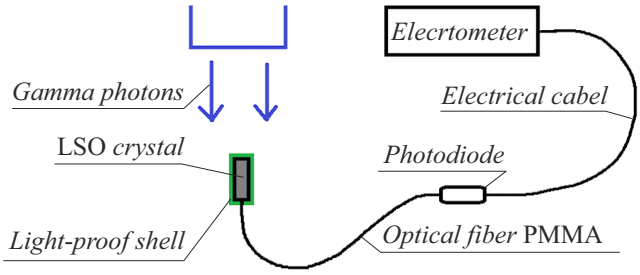

Figure 1. Diagram of the scintillation detector.

conditions using the Varian Unique electron accelerator and the Sun Nuclear 3D SCANNER water phantom with an embedded two-channel PC Electrometer [19,20].

The radiation beam is represented by a continuous spectrum of deceleration photons with bombarding electrons' maximum energy of 6 MeV.

Two detectors were fabricated: based on the LSO crystals of the size $3 \times 3 \times 10$ mm and $3 \times 3 \times 15$ mm. Each detector consisted of the crystal optically coupled, via a special glue with a refractive index 1.5−1.6, with a polymethyl methacrylate optical fiber of the 120 cm length and the 3 mm diameter, which was designed to transmit the light signal to a FD265A photodiode with the sensitive area 1.45×1.45 mm. At the same time, all connections were additionally protected by a heat shrink tube in order to provide mechanical stability of light insulation, while the crystals were placed in water-equivalent opaque plastic caps of the 1 mm thickness. A diagram of the detector is shown in Fig. 1.

An optical fiber between the scintillator and the photodiode is designed for removing the photodiode out of a radiation field. It is required for two reasons: the photodiode has a metal case that creates a powerful flux of secondary electrons, which affects measurement results; being a semiconductor, the photodiode itself generates a current when it is hit by gamma photons. The optical fiber makes it possible to almost completely avoid influence of IR on the photodiode and, correspondingly, on the measurement results.

The photocurrent in a point measurement mode was recorded by a clinical dosimeter Dose-1 in the electrometer mode and an instrument error of the measurements was 0.5 % [21].

Calibration measurements started from determining basic characteristics of the detector, including a dependence of photocurrent on dose power within the range 1−6 Gy/min with the step of 1 Gy/min. The measurements were performed on a table for radiotherapeutic procedures at the distance of 100 cm to a gantry, the field was 10×10 cm, and the photodiode was at a distance of 120 cm to the radiation field. It also included measurements of a dark current of the photodiode both with the accelerator turned off as well as during its operation, but with the detector outside the radiation field, thereby making it possible to estimate a contribution by scattered radiation to total noise of the system. Additionally, a coefficient of detector nonlinearity was calculated — nonlinearity of photocurrent variation with variation of power and the dose.

Influence of intrinsic radioactivity of the crystals was measured by measuring a signal from the detector without the radiation beam in three days of fluorescence. Besides, in order to determine influence of scintillation of polymethyl methacrylate, the optical fiber was placed in the radiation field without the glued crystal at all possible dose powers (1−6 Gy/min with the step of 1 Gy/min).

In order to estimate the fluorescence lifetime of the crystal, afterglow of the crystal was measured in 10 min of irradiation at power of 5 Gy/min, wherein the signal was recorded with the intervals from 15 to 60 s for 15 min after termination of irradiation.

The main dosimetric measurements were performed in the water phantom, where the detector was placed with a step of 1 mm along the depth from the surface up to 25 cm for plotting a curve of depth distribution of the dose and then laterally at the depth of 10 cm for obtaining a beam profile 3×3 cm. Comparison with the semiconductor detector Sun Nuclear EDGE and the ionization chamber Sun Nuclear Ion Chamber 125c was performed in the same conditions [22,23].

3. Results

3.1. Simulation results

Simulation by the Monte Carlo method in Geant4 made it possible to obtain a detailed pattern of interaction of IR with the LSO crystal and subsequent formation of optical photons, wherein a key result was detection of a clear dependence of efficiency of light output on geometric parameters of the crystal and energy of incident radiation. With the small crystal lengths, a part of gamma quanta exits its overall dimensions, thereby resulting in reduction of energy release. At the same time, with the increase of the crystal length, losses during photon re-reflection increases. For photons of 511 keV the maximum efficiency of detection was achieved with the crystal length of 8 mm, whereas the higher energies exhibited a regular shift of the maximum of light output towards the bigger lengths. It is explained by the increased depth of penetration of high-energy photons and a need of full absorption of their energy within the scintillator volume (Fig. 2).

Special attention during simulation was paid to processes of light losses in a signal transmission system. The PMMA optical fiber of the 120 cm length had total signal attenuation by 18.9 % specified, and it included 12.3 % of losses for absorption in the material and 6.6 % for re-reflections at interfaces. This ratio necessitates use of specialized lightguides with improved characteristics of transmittance within the scintillator radiation range (420 nm) in order to improve total efficiency of the system. Simulation of spatial distribution of energy release in the crystal identified

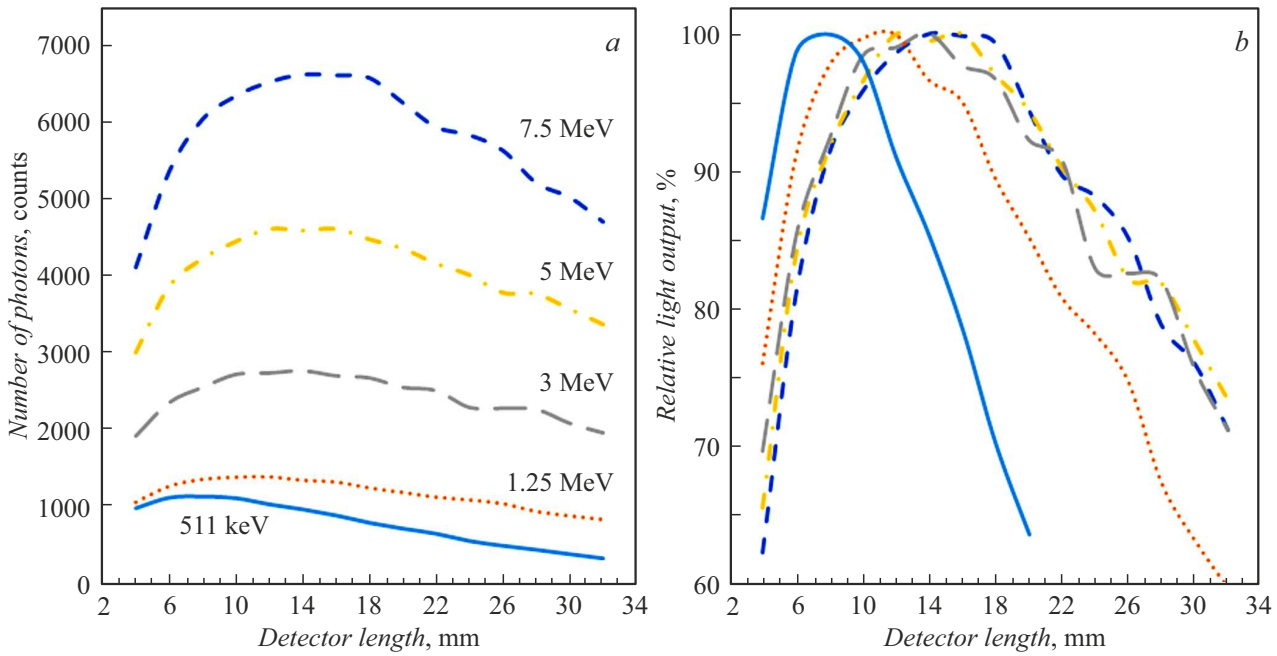

Figure 2. *a* — Dependence of the number of the detector-recorded photons on the length of the scintillation crystal and energy of gamma quanta; *b* — Dependence of relative light output of the scintillator on energy of gamma quanta and the crystal length.

significant nonuniformity that was especially pronounced for the high energies (5–7.5 MeV), where the maximum of ionization is shifted deep into the crystal, forming a typical profile with a sharp increase of an excitation density at the first millimeters and a gradual drop to the opposite face end. It shall be taken into account when interpreting experimental data and designing signal correction algorithms.

3.2. Results of experimental verification

Determination of the main characteristics of the detector resulted in specifying a direct dependence of photocurrent on dose power. A signal/noise ratio for LSO $3 \times 3 \times 10$ mm is 250, and for $3 \times 3 \times 15$ mm it is 450. About 95 % of the noise signal was allocated to photocurrent from scattered radiation in an accelerator canyon, which unavoidably hits the photodiode. Linearity of a detector response within the power range 1–6 Gy/ was confirmed by a high coefficient of determination ($R_2 = 0.977$) when measuring the dependence of photocurrent on dose power, where a charge value at 1 Gy remained stable within 2862–2880 pC (for the crystal $3 \times 3 \times 10$ mm), demonstrating the deviation of at most 1 %. At the same time, the nonlinearity coefficient calculated as a relative deviation from the ideal straight line was progressively increasing from 0.59 % at 2 Gy/min to 3.52 % at 6 Gy/min, which is related to gradual saturation of the photodiode at high levels of the signal (Fig. 3).

We could not estimate influence of intrinsic radioactivity of the crystals on the measurement results, since the electrometer used did not record statistically significant

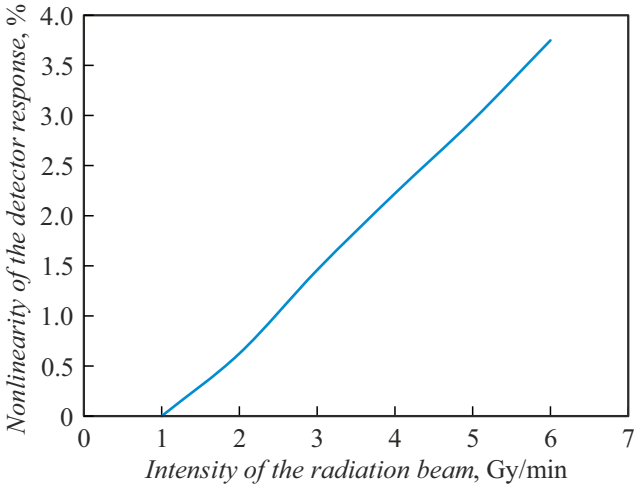

Figure 3. Variation of the nonlinearity coefficient of the detector with the increase of radiation power.

deviations of power of the recorded photocurrent when connecting the detectors without their preliminary irradiation. External interference to the electrometer did not exceed 0.05 pA.

When studying angular sensitivity, signal changes did not exceed 1 %, thereby indicating isotropicity of light yield and absence of a pronounced dependence on crystal orientation in the radiation field.

Afterglow of the smaller LSO crystal in 1 min after 10 min irradiation at 5 Gy/min was 0.41 and 0.30 pA in 15 min, decreasing as per the logarithmic law, as shown in

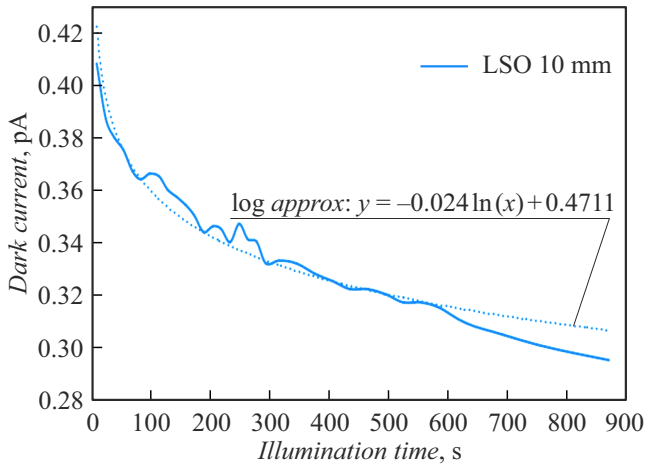

Figure 4. Afterglow of the LSO crystal.

Fig. 4. This factor shall be taken into account during serial measurements with short intervals between exposures.

In order to estimate influence of PMMA scintillation on the general level of photocurrent, the optical fiber without the crystal was irradiated. 10 cm of the optical fiber was in the radiation field, which corresponds to 0.7 cm^3 of polymethyl methacrylate: this volume of the optical fiber can be under the beam during the measurements. No photocurrent from scintillation of the plastic has been recorded outside the dependence on dose power, which is related to its low light yield without adding activators as well as insensitivity of the photodiode to light in the UV range, which comprises the maximum of radiation.

3.3. Results of dosimetry in the water phantom

According to the results of dosimetry in the water phantom, the detectors demonstrated spatial resolution when measuring the beam profile, which was comparable to the detector Sun Nuclear EDGE, as it is clear in Fig. 5.

The measurement results were normalized to the maximum for visual comparison of the results. The level of the signal from the smaller crystal is higher in the shadow of the radiation beam due to a worse signal-to-noise ratio: background exposure of the photodiode to scattered radiation in the accelerator canyon affects the measurement results.

The depth distributions of the dose, which are obtained when scanning from the water surface to 25 cm with a step of 1 mm, demonstrated the maximum of ionization of the smaller crystal at the depth (11 ± 0.1) mm and at (12 ± 0.1) mm for the bigger crystal, with a reference value of 14 mm, which can be seen in Fig. 6. The Figure clearly demonstrates different forms of the graphs, thereby indicating a different behavior of the scintillators and the ionization chamber under conditions of the radiation flux changing around the detector. Due to their design, the scintillation detectors absorb more energy and output a

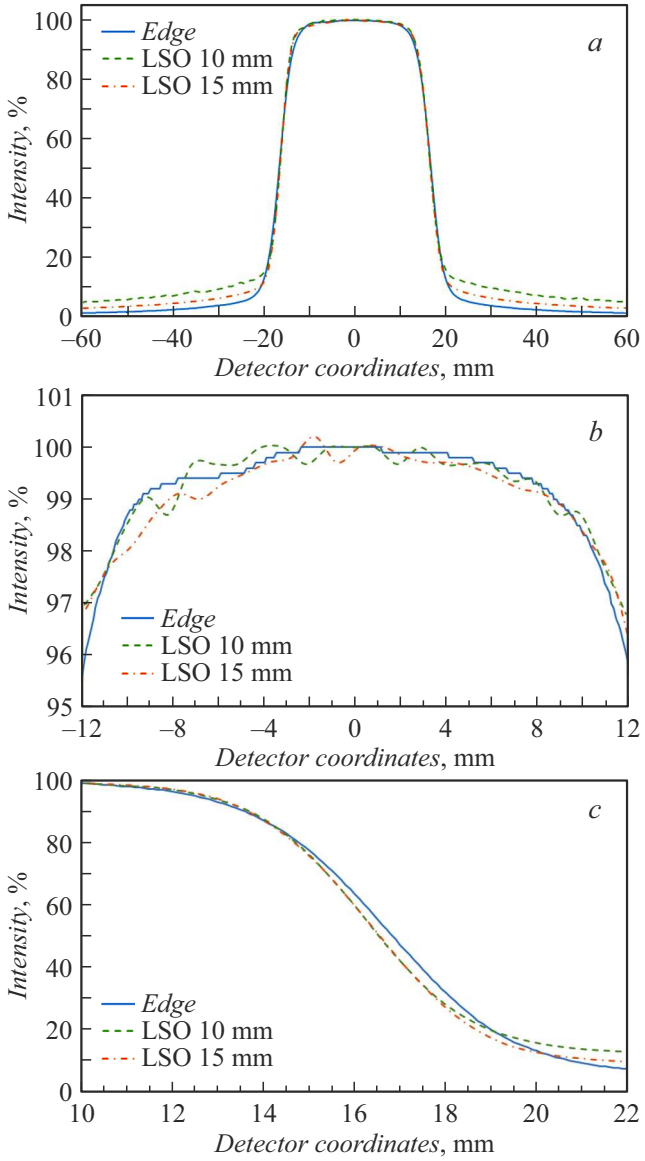

Figure 5. Results of dosimetry at the 10 cm depth in the radiation field 3 × 3 cm: *a* — the general view, *b* — the central part of the field, *c* — the shadow part of the beam.

higher signal, whereas in reality the real distribution of dose power with the depth is close to readings of the ionization chamber, which unlike the crystals has almost no effect on the radiation flux. The better results of measurement of depth dose power can be demonstrated by organic (tissue-equivalent) scintillators. But due to lower light yield and the smaller density they will emit much less light, which is a serious limitation when reducing the sensitive volume.

The comparison with the commercial detector Sun Nuclear EDGE and the ionization chamber SNC125 demonstrated both advantages as well as limitations of the designed system. On the one hand, the LSO detector demonstrated good spatial resolution when scanning a beam shadow region due to the small sensitive area and absence of the

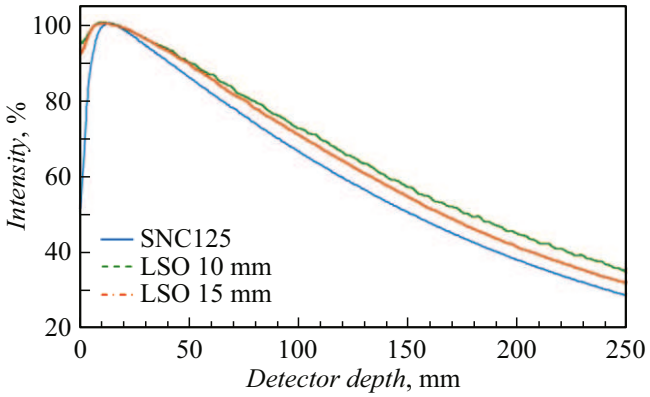

Figure 6. Results of measurement of the depth distribution of dose power.

metal case that creates additional scattering. On the other hand, due to specific features of the design of the detectors the depth distribution of the dose is incorrectly recorded, thereby excluding use of the likewise-designed scintillation detectors when measuring the dependence of dose power on the depth.

Conclusion

The scintillation detector based on the LSO crystal and designed for tasks of clinical dosimetry has been studied to make some crucial conclusions that are important for designing the methods of precise radiotherapy. The key achievement was experimental confirmation of usability of the scintillation detectors, which is especially critical for the modern methods of conformal irradiation and stereotaxic radiosurgery, which require submillimeter accuracy of dosimetry monitoring. The obtained results demonstrate that the scintillators can become a base for the new-generation dosimetry instruments that combine high accuracy of measurements with radiation resistance and temperature stability. At the same time, the most important technological advantage is that it is possible to create miniature detector assemblies with the sensitive volume below 0.1 cm^3, which can not be achieved for the traditional ionization chambers.

The following conclusion can be made by analysis of the experimental data: the scintillation detectors can be used in relative clinical dosimetry except for measurements of the dependence of the dose on the depth.

The identified advantages of the scintillation detectors may include measurement accuracy that is comparable to the commercial detector Sun Nuclear EDGE during horizontal scanning of the radiation beam, and the signal-to-noise ratio that is enough for selecting a „clear“ signal in the proven design of the detector without using a PMT. The disadvantages are: heavy influence of the scintillator on the radiation flux therearound, which makes it impossible to correctly measure the depth distribution of the dose in the water phantom; a need of taking into account the radiation dose received by the detector and varying light yield, since the crystal degrades due to accumulation of radiation defects (it does not matter in relative dosimetry). A disadvantage of the specific tested samples is also a silicon photodiode, whose sensitivity in the spectrum blue-violet range (380–420 nm) is at the level of 5 %–10 % of the maximum one. Selection of a more suitable photodiode will make it possible to significantly improve the signal-to-noise ratio, thereby positively affecting the signal quality.

Conflict of interest

The authors declare that they have no conflict of interest.

References

[1] S. Gundacker, E. Auffray, K. Pauwels, P. Lecoq. Phys. Med. Biol., **61** (7), 2802 (2016). DOI: 10.1088/0031-9155/61/7/2802

[2] S. Siegel, M. Eriksson, A.A. Carey, L. Eriksson, R. Nutt. *Polyphosphoric acid etching of LSO crystals for improved light output, energy resolution and light transmission*. 2000 IEEE Nuclear Science Symposium. Conference Record (Lyon, France, 2000), v. 2, p. 14/60. DOI: 10.1109/NSSMIC.2000.950027

[3] H. Rothfuss, L. Byars, M.E. Casey, M. Conti, L. Eriksson, C. Michel. Nucl. Instrum. Methods Phys. Res. Section A: Accelerators, Spectrometers, Detectors and Associated Equipment, **580** (2), 1087 (2007). DOI: 10.1016/j.nima.2007.06.067

[4] R. Mao, C. Wu, L. Dai, S. Lu. J. Crystal Growth, **368**, 97 (2013). DOI: 10.1016/j.jcrysgro.2013.01.038

[5] J. Chen, L. Zhang, R. Zhu. Nucl. Instrum. Methods Phys. Res. Section A: Accelerators, Spectrometers, Detectors and Associated Equipment, **572**, 218 (2007). DOI: 10.1016/j.nima.2006.10.213

[6] E. Auffray, A. Borisevitch, A. Gektin, Ia. Gerasymov, M. Korjik, D. Kozlov, D. Kurtsev, V. Mechinsky, O. Sidletskiy, R. Zoueyski. Nucl. Instrum. Methods Phys. Res. Section A: Accelerators, Spectrometers, Detectors and Associated Equipment, **783**, 117 (2015). DOI: 10.1016/j.nima.2015.02.038

[7] S. Lam, M. Gascón, S. Podowitz, S. Curtarolo, R.S. Feigelson. IEEE Transactions on Nucl. Sci., **60** (2), 993 (2013). DOI: 10.1109/TNS.2012.2234136

[8] F. Ahmadov, A. Sadigov, Yu.Yu. Bacherikov, O. Okhrimenko, K. Isayev, M. Holik, T. Slavicek, F. Mamedov, G. Ahmadov, A. Mammadli, R. Akbarov, J. Nagiyev, D. Berikov, S. Nuruyev, Z. Sadygov, Yu. Shitov, S.I. Lyubchyk, S.B. Lyubchyk. Sci. Rep., **15**, 2823 (2025). DOI: 10.1038/s41598-025-85845-y

[9] G. Rovera, L. Urso, F. Stracuzzi, R. Laudicella, V. Frantellizzi, Ch. Cottignoli, M. Gazzilli, P. Guglielmo, S. Panareo, L. Evangelista, A. Filice, L. Burroni. Accreditamento Management — HTA AIMN Working Group. Clin Transl. Imaging, **12**, 743 (2024). DOI: 10.1007/s40336-024-00650-3

[10] C.M. Pepin, P. Berard, A.-L. Perrot, C. Pepin, D. Houde, R. Lecomte, C.L. Melcher, H. Dautet. IEEE Transactions Nucl. Sci., **51** (3), 789 (2004). DOI: 10.1109/TNS.2004.829781

[11] I. Alberts, J.N. Hünermund, G. Prenosil, C. Mingels, K.P. Bohn, M. Viscione, A. Rominger. Europ. J. Nucl. Med. Molecular Imaging, **48** (8), 2395 (2021). DOI: 10.1007/s00259-021-05282-7
[12] G.A. Prenosil, H. Sari, M. Fürstner, A. Afshar-Oromieh, K. Shi, A. Rominger, M. Hentschel. J. Nucl. Med., **63** (3), 476 (2022). DOI: 10.2967/jnumed.121.261972
[13] S.A. Zein, N.A. Karakatsanis, M. Conti, S.A. Nehmeh. IEEE Transactions on Radiat. Plasma Med. Sci., **5** (3), 331 (2020). DOI: 10.1109/TRPMS.2020.3034676
[14] M. Dadgar, J. Maebe, Akl M. Abi, B. Vervenne, S. Vandenberghe. *System characteristics comparison of the Walk-Through Total-Body PET and the Biograph Vision Quadra PET/CT* (Preprint, 2023). DOI: 10.21203/rs.3.rs-2742020/v1
[15] Y. Yang, S.S. James, Y. Wu, H. Du, J. Qi, R. Farrell, P.A. Dokhale, K.S. Shah, K. Vaigneur, S.R. Cherry. Phys. Med. Biol., **56** (1), 139 (2011). DOI: 10.1088/0031-9155/56/1/009
[16] Y.C. Tai, A. Ruangma, D. Rowland, S. Siegel, D.F. Newport, P.L. Chow, R. Laforest. J. Nucl. Med.: Official Publication, Society Nucl. Med., **46** (3), 455 (2005).
[17] S.I. Ziegler, B.J. Pichler, G. Boening, M. Rafecas, W. Pimpl, E. Lorenz, N. Schmitz, M. Schwaiger. Europ. J. Nucl. Med., **28** (2), 136 (2001). DOI: 10.1007/s002590000438
[18] F. Ahmadov, A. Sadigov, Y.Y. Bacherikov, O. Okhrimenko, K. Isayev, M. Holik, T. Slavicek, F. Mamedov, A. Ahmadov, A. Mammadli, R. Akbarov, J. Nagiyev, D. Berikov, S. Nuruyev, Z. Sadygov, Y. Shitov, S.I. Lyubchyk, S.B. Lyubchyk. Scientif. Reports, **15** (1), 2823 (2025). DOI: 10.1038/s41598-025-85845-y
[19] Electron accelerator Varian Unique: https://www.varian.com/en-ca/products/radiotherapy/treatment-delivery/unique
[20] Water phantom Sun Nuclear 3D SCANNER: https://www.sunnuclear.com/products/3d-scanner
[21] Clinical dosimeter Dose-1: https://universalenterprisespk.com/medical-equipment/iba-dosimetry-dose01-brochure.pdf
[22] Semiconductor detector Sun Nuclear EDGE: https://www.sunnuclear.com/products/edge-detector
[23] Ionization chamber SNC125: https://www.sunnuclear.com/Products/Snc125c-snc350p-snc600c

Translated by M.Shevelev